Engineering Structures 244 (2021) 112759

Contents lists available at ScienceDirect

Engineering Structures

journal homepage: www.elsevier.com/locate/engstruct

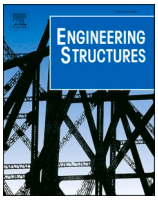

Free vibration of viscoelastically supported beam bridges under moving loads: Closed-form formula for maximum resonant response

Abbas Zangeneh [a,c,*], Pedro Museros [b], Costin Pacoste [a,c], Raid Karoumi [a]

[a] Division of Structural Engineering and Bridges, KTH Royal Institute of Technology, Stockholm, Sweden
[b] Universitat Politecnica de Valencia, Departamento de Mecanica de Medios Continuosy Teoria de Estructuras, 46022 Valencia, Spain
[c] ELU Konsult AB, Stockholm, Sweden

ARTICLE INFO

Keywords:
Railway bridges
Soil-Structure Interaction
Viscoelastic supports
Discrete Model
Moving loads
Resonance
Train signature

ABSTRACT

In this paper, a closed-form approximate formula for estimating the maximum resonant response of beam bridges on viscoelastic supports (VS) under moving loads is proposed. The methodology is based on the discrete approximation of the fundamental vertical mode of a non-proportionally damped Bernoulli–Euler beam, which allows the derivation of closed-form expressions for the fundamental modal characteristics and maximum amplitude of free vibration at the mid-span of VS beams. Finally, an approximate formula to estimate maximum resonant acceleration of VS beams under passage of articulated trains has been proposed. Verification studies prove that the approximate closed-form formula estimates the resonant peaks with good accuracy and is a useful tool for preliminary assessment of railway beam bridges considering the effect of soil-structure interaction at resonance. In combination with the use of full train *signatures* through the *Residual Influence Line* (LIR) method, the proposed solution yields good results also in the lower range of speeds, where resonant sub-harmonics are more intensely reduced by damping.

1. Introduction

The train-induced vibration analysis of railway bridges has been extensively studied by many researchers, including Frýba [1], Weaver et al. [2], Olsson [3], Yang et al. [4], Michaltsos [5] and Savin [6], among others [7–13]. Due to the periodic nature of the train loading, a railway bridge may experience resonance effects. Resonance in railway bridges occurs when the train loading frequency, i.e. the ratio between the train speed and the characteristics axle distance, coincides with the fundamental frequency of the bridge [1,14–15]. Under resonance condition, the bridge decks may experience extreme vibration levels due to the incessant accumulation of the free-vibration oscillations generated by the consecutive moving loads. On the other hand, the cancellation phenomenon implies that either the free vibrations of the bridge caused by each single load cancel at particular speeds, or the free vibrations caused by the successive moving loads negate each other. [6,7,12,13].

A number of researchers have studied the moving load problem for simply supported (SS) beams and elastically supported (ES) beams with the aim of finding approximate closed-form formulas that can estimate the peak resonant response of the system under moving load. Frýba [8] proposed approximate formulas for estimating the amplitudes for maximum displacement, acceleration and bending moment of a simply supported bridge due to resonance of the fundamental mode. Savin [6] derived approximate expressions to compute the peak vertical deflection and acceleration of beams with classical boundary conditions, introducing a spectrum of the train which is almost equal to the so-called dynamic signature presented by the LIR (Residual Influence Line) method in the framework of the ERRI D-214 Committee [14]. The resonance and cancellation phenomena of ES beams has been analysed by Yau et al. [10] and Yang et al. [11] using an approximate expression of the first bending mode. Xia et al. [12] studied in depth the different cancellation and resonance phenomena, both for single loads and series of successive loads. Museros et al. [13] comprehensively studied the maximum free vibration and cancellation conditions for SS and ES beams under a moving load, and developed as well an approximate formula to estimate peak vertical accelerations of simply supported beams under passing articulated trains.

In all aforementioned previous solutions, the classical boundary conditions for the beam are considered, assuming that the system is proportionally damped and characterized by classical normal modes. In the presence of foundation damping as in a viscoelastically supported (VS) beam, however, this approximation may not be valid as the energy

* Corresponding author.
E-mail address: abbaszk@kth.se (A. Zangeneh).

https://doi.org/10.1016/j.engstruct.2021.112759
Received 10 November 2020; Received in revised form 13 April 2021; Accepted 20 June 2021
Available online 30 June 2021

dissipation is not distributed uniformly over the system, rendering the modes non-classical and complex [16,17]. The frequency content and amplitude of the vibrations in the resonant response of railway bridges is governed by the modal characteristics (natural frequency and damping ratio) of the structural system. Hence, to predict the resonant response with reasonable accuracy, it is important to properly estimate the modal characteristics of the structural system, considering the effect of the flexibility and dissipation capacity of the supporting foundation-soil system. In this regard, several studies on the dynamic soil-structure analysis of railway beam bridges [18–22] revealed that the modal properties and resonant response of bridges might be considerably affected by the flexibility and dissipation capacity of the supporting foundation-soil system.

Romero et al. [18] studied the effect of Soil-Structure Interaction (SSI) on the resonance response of a simple beam bridge supported by half-space medium using a fully three dimensional (3D) multi-body boundary element-finite element model formulated in the time domain. The authors concluded that both the period and damping ratio of the fundamental bending mode of the system are higher when SSI is considered. On the basis of numerical simulations, Doménech et al. [19] studied the effect of SSI on the fundamental modal properties and maximum free vibration and cancellation phenomena of simple beams founded on a homogenous half-space medium under a single moving load by using a 3D Boundary Element-Finite Element coupled model (BEM-FEM). The analysis showed that considering soil effects leads to a reduction of the bridge maximum free vibration amplitudes and train-induced resonant response as a consequence of the inherent damping of the soil due to wave radiation. The study concluded that the effect of SSI increases as the ratio between the beam flexural stiffness and the foundation-soil stiffness becomes higher. In [23], Svedholm et al. developed an analytical solution for complex mode superposition analysis of a Bernoulli-Euler beam supported by viscoelastic supports which used to study the effects of SSI on modal properties of reinforced concrete bridges with ballasted tracks supported on half-space medium [20]. The results presented in the study showed that the expected foundation damping ratio for the 1st bending mode of the system is between 0.1% and 6% for a long span bridge ($L = 60$ m) supported by a dense soil and for a short span bridge ($L = 5$ m) supported by a loose soil, respectively. Zangeneh et al. [21] proposed closed-form expressions for calculating the dynamic characteristics of the fundamental bending mode of single span beam bridges on viscoelastic supports using a 2 degree of freedom (2DoF) discrete model. This model was used to study the effect of the dynamic stiffness of the foundation on the modal parameters (e.g. natural frequency and damping ratio) of railway beam bridges. It was shown that the effect of SSI depends not only on the ratio between the flexural stiffness of the bridge and the dynamic stiffness of the foundation-soil system but also on the ratio between the resonant frequency of the soil layer and the fundamental frequency of the bridge. If the fundamental frequency of the beam is lower than the resonance frequency of the supporting soil stratum, the radiation damping capacity of the soil deposit is almost zero. Consequently, the dynamic response of the system becomes close to an elastically supported beam and the effect of supports flexibility may become detrimental [11,22].

To investigate the effect of soil-structure interaction on the resonant response of railway beam bridges in a systematic manner, the derivation of closed-form formulas for computing fundamental modal characteristics and free vibration amplitude of the bridge-foundation-soil system is useful. Hence, the objective of this paper is to propose a novel closed-form expression for computing the maximum free vibration amplitude of viscoelastically supported beams traversed by a single load as shown in Fig. 1. The methodology based on the approximation of a VS beam by a two DoF discrete model [21] is used as a starting point. Subsequently, an approximate formula to estimate maximum resonant acceleration of VS beams under the passage of articulated trains is proposed. The accuracy and applicability of the proposed closed-form expressions will be verified through comparison with the analytical solutions.

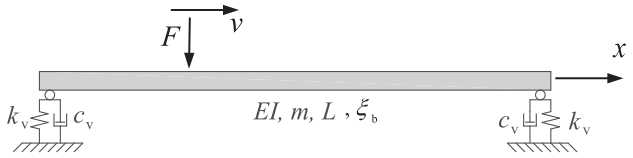

Fig. 1. Moving load problem of a viscoelastically supported (VS) beam.

Certainly, the train-induced vibration analysis of VS beams could be solved by a commercial FE package; however, the proposed closed-form expressions can be used to: (a) accurately compute the fundamental modal characteristics, maximum free vibration amplitude and cancellation of viscoelastically supported beams at very low computational cost, (b) gain physical insight into the nature of SSI effects by studying how resonant response of beam bridges changes when SSI is included or excluded, (c) approximate the peak resonant acceleration of beam bridges generated by high-speed trains straightforwardly in the preliminary stages of bridge design, considering SSI effect, and (d) provide a computationally efficient tool suitable for screening of railway bridge networks using probabilistic analysis and Monte Carlo simulations.

This paper is organized as follows. In section 2, a brief overview of the governing equations of the 2DoF discrete model proposed in [21] for vibration analysis of viscoelastically supported beams and closed-form expressions for computing fundamental modal characteristics of the studied system is given. Then, the derivation of a novel closed-form expression for estimating peak mid-span free vibration amplitude of a VS beam passing by a single moving load is presented, followed by the verification of the proposed solution against analytical solutions. Section 3 proposes an approximate formula for estimating the maximum mid-span acceleration due to resonance of the fundamental mode of a VS beam passing by regular or articulated trains; also, the role of shear deformation and additional bending modes is discussed in the last subsection therein. In Section 4, the practical applicability and validity of the proposed approximate formula is examined for different case studies. Concluding remarks are presented in Section 5.

2. Free vibration of viscoelastically supported beam under a single moving load.

As shown in Fig. 1, a single–span 2D Bernoulli-Euler beam supported by two viscoelastic supports of stiffness k_v and damping c_v at the two ends is considered. The beam is traversed by a constant valued load F moving at constant speed v and assumed to have a length L and a uniform cross-section with flexural rigidity EI, mass per unit length m, and structural damping ratio ξ_b.

2.1. Proposed discrete model, equations of motion and system matrices

As shown by Zangeneh et al. [21], the fundamental vertical bending mode shape of the studied continuous system can be well approximated

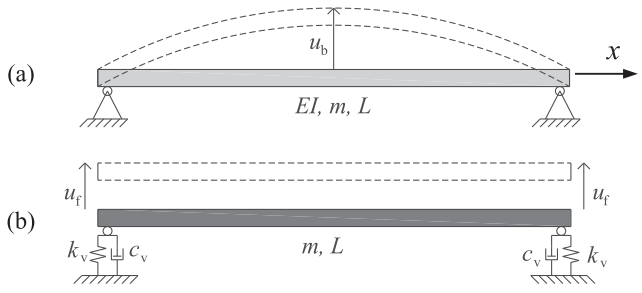

Fig. 2. Model of free vibration mode shape of viscoelastically supported beam as a superposition of (a) simply supported beam and (b) rigid beam on viscoelastic supports.

by the superposition of the flexural sine mode of a simply supported beam (Fig. 2a) and the rigid body mode shape of the beam supported by viscoelastic supports, as shown in Fig. 2b. Hence, the displacement field $u(x,t)$ of the equivalent 2 degrees of freedom system can be expressed as Eq. (1).

$$u(x,t) = \boldsymbol{N}.\boldsymbol{d} \cong \begin{bmatrix} 1 & sin(\frac{\pi x}{L}) \end{bmatrix} \begin{Bmatrix} u_f(t) \\ u_b(t) \end{Bmatrix} \tag{1}$$

where **N** represents the vector of assumed shape functions, **d** is the vector of generalized coordinates of the vibration shapes, and u_f (t) and u_b (t) are the displacements at the supports and the mid-span, respectively.

Following the procedure in [21], the equation of motion for the free response of the discrete 2DoF system can be written as follows:

$$\boldsymbol{M}\ddot{\boldsymbol{d}} + \boldsymbol{C}\dot{\boldsymbol{d}} + \boldsymbol{K}\boldsymbol{d} = 0 \tag{2}$$

where

$$\boldsymbol{d} = \begin{Bmatrix} u_f(t) \\ u_b(t) \end{Bmatrix}, \boldsymbol{M} = mL\begin{bmatrix} 1 & 1/\pi \\ 2/\pi & 1/2 \end{bmatrix}, \boldsymbol{C} = \begin{bmatrix} 2c_v & 0 \\ 0 & 0 \end{bmatrix},$$
$$\boldsymbol{K} = \begin{bmatrix} 2k_v & 0 \\ 0 & \pi^4 EI/2L^3 \end{bmatrix}$$

It should be noted that in the derivation of system matrices, the structural damping of the beam is neglected and only the foundation damping is considered. Structural damping is later introduced in the following subsection. Detailed information about the derivation of system matrices can be found in [21]. Employing similar superposition assumption for the fundamental vertical mode shape (see Fig. 2), the governing differential equation of motion for the 2DoF linear system under a single moving load can also be written as Eq. (3).

$$\boldsymbol{M}\ddot{\boldsymbol{d}} + \boldsymbol{C}\dot{\boldsymbol{d}} + \boldsymbol{K}\boldsymbol{d} = -F\boldsymbol{P}(t) \tag{3}$$

where $\boldsymbol{P}(t) = \begin{bmatrix} 1 & sin\frac{\pi vt}{L} \end{bmatrix}^{\mathrm{T}}$.

2.2. Fundamental frequency, modal damping ratio and complex eigenvector

By assuming a solution for the free vibration of the system of the form $u = \phi e^{\lambda t}$, the complex modal characteristics of the discrete system for mode n can be found as the solution of the quadratic eigenproblem in Eq. (4).

$$\left[\boldsymbol{K} + \lambda_n \boldsymbol{C} + \lambda_n^2 \boldsymbol{M}\right]\boldsymbol{\varphi}_n = 0 \tag{4}$$

where λ_n and $\boldsymbol{\varphi}_n^{\mathrm{T}} = \begin{bmatrix} \phi_{f,n} & \phi_{b,n} \end{bmatrix}$ are the complex-valued eigenvalue and corresponding eigenvector of mode n. Provided that the desired mode of vibration is underdamped —as in most practical applications—, eigenvalues always occur as pairs of complex conjugate roots [24] as in Eq. (5), and thus the free response is a decaying oscillatory motion.

$$\lambda_n = -\xi_n\omega_n \pm i\omega_n\sqrt{1-\xi_n^2} \tag{5}$$

where ω_n denotes the undamped natural frequency and ξ_n is the modal damping ratio.

Zangeneh et al. [21] showed that by introducing the system matrices from Eq. (2) into Eq. (4) and analytically solving a quartic polynomial equation, the closed-form expressions for the natural frequency and modal damping ratio for fundamental vertical mode of studied system (disregarding the structural damping of the beam itself) can be obtained as Eq. (6) and Eq. (7), respectively.

$$\omega_0 = \sqrt{\left(\eta|S| - \frac{\pi^2\beta}{2(\pi^2-8)\gamma}\right)^2 + |S|^2 + \frac{p}{2} + \eta\frac{q}{4|S|}} \tag{6}$$

$$\xi_0 = \frac{1}{\omega_0}\left(\frac{\pi^2\beta}{2(\pi^2-8)\gamma} - \eta|S|\right) \tag{7}$$

where subscript "0" denotes the fundamental mode (lowest unerdamped vertical mode) of the system and $\gamma, D, \beta, p, q, S, \eta$ are functions of geometrical and material properties of the beam and its viscoelastic supports, as presented in Appendix A. Detailed information about the derivation of closed-form expressions can be found in [21].

As it was mentioned before, in the derivation of the closed-form expressions, the structural damping of the beam is disregarded. Subsequently, the effect of structural damping can be approximately introduced into Eq. (7) [25], and thus the total modal damping ratio for the fundamental vertical mode of system obtained as per Eq. (8).

$$\xi_0 \approx \xi_b\left(\frac{\omega_0}{\omega_0^{SS}}\right)^2 + \frac{1}{\omega_0}\left(\frac{\pi^2\beta}{2(\pi^2-8)\gamma} - \eta|S|\right) \tag{8}$$

where ξ_b and ω_0^{SS} are the structural damping ratio and the fundamental natural frequency of the beam on ideal simple supports with zero flexibility, respectively. The validity of the preceding assumptions for the analysis of actual simply-supported bridges will be demonstrated in Section 2.5.2.

Having closed-form expressions for ω_0, ξ_0 and thus λ_0, the ratio between complex eigenvectors of the fundamental vertical mode can be easily obtained as a solution of the Eq. (4):

$$\frac{\phi_{f,0}}{\phi_{b,0}} = -\frac{2mL\lambda_0^2}{\pi(2k_v + 2\lambda_0 c_v + mL\lambda_0^2)} \tag{9}$$

With all complex modal characteristics of the desired vibration mode in hand, obtaining an analytical solution to the resonant response of beam at mid-span by using complex mode superposition is now possible.

2.3. Complex mode superposition

First, the governing differential equation of motion of 2DoF discrete system in Eq. (3) is transformed into the state-space form as following:

$$\boldsymbol{A}\dot{\boldsymbol{y}} + \boldsymbol{B}\boldsymbol{y} = -F\boldsymbol{Q}(t) \tag{10}$$

where $\boldsymbol{y} = \begin{bmatrix} \dot{\boldsymbol{d}} \\ \boldsymbol{d} \end{bmatrix}$, $\boldsymbol{A} = \begin{bmatrix} \boldsymbol{0} & \boldsymbol{M} \\ \boldsymbol{M} & \boldsymbol{C} \end{bmatrix}$, $\boldsymbol{B} = \begin{bmatrix} -\boldsymbol{M} & \boldsymbol{0} \\ \boldsymbol{0} & \boldsymbol{K} \end{bmatrix}$, $\boldsymbol{Q}(t) = \boldsymbol{Q}(t) = \begin{bmatrix} \begin{bmatrix} 0 \\ 0 \end{bmatrix} \\ \boldsymbol{P}(t) \end{bmatrix}$

Letting $\boldsymbol{d}_n = \boldsymbol{\varphi}_n e^{\lambda_n t}$ for n^{th} mode of vibration results in $\boldsymbol{y}_n = \boldsymbol{\psi}_n e^{\lambda_n t}$ where $\boldsymbol{\psi}_n = \begin{bmatrix} \lambda_n\boldsymbol{\varphi}_n \\ \boldsymbol{\varphi}_n \end{bmatrix}$ is the state complex eigenvector of mode n, of dimensions 4 by 1.

Provided that the studied system has always 4 sets of unique non-repeatable eigenvalues, the state complex eigenvector matrix $\boldsymbol{\Psi}$ is invertible and the equation of motion in state-space form can be converted to the modal basis as follows:

$$\boldsymbol{\Psi}^{\mathrm{T}}\boldsymbol{A}\boldsymbol{\Psi}\dot{\boldsymbol{y}} + \boldsymbol{\Psi}^{\mathrm{T}}\boldsymbol{B}\boldsymbol{\Psi}\boldsymbol{y} = -F\boldsymbol{\Psi}^{\mathrm{T}}\boldsymbol{Q}(t) \tag{11}$$

As proved by Zhao et al. [26], the uncoupled equation of motion for mode n can be then written as Eq. (12) by letting $\boldsymbol{y} = \boldsymbol{\Psi}\boldsymbol{z}$ and substituting it into Eq. (11).

$$\dot{z}_n(t) - \lambda_n z_n(t) = -\frac{F}{\alpha_n}\boldsymbol{\varphi}_n^{\mathrm{T}}\boldsymbol{P}(t) \tag{12}$$

where **z** is the modal amplitude vector, z_n is the n^{th} modal amplitude and $\alpha_n = 2\lambda_n\boldsymbol{\varphi}_n^{\mathrm{T}}\boldsymbol{M}\boldsymbol{\varphi}_n + \boldsymbol{\varphi}_n^{\mathrm{T}}\boldsymbol{C}\boldsymbol{\varphi}_n$.

2.4. Amplitude of the free vibration due to the fundamental vertical mode

For the fundamental vertical mode, the differential equations that govern the modal amplitude of the system can be written as follows:

$$\dot{z}_0(t) - \lambda_0 z_0(t) = -\frac{F}{\alpha_0}\left(\phi_{f,0} + \phi_{b,0} sin\Omega t\right), \quad 0 \leqslant t \leqslant L/v \tag{13a}$$

$$\dot{z}_0(t) - \lambda_0 z_0(t) = 0, \quad t > L/v \tag{13b}$$

where $\Omega = \frac{\pi v}{L}$ and $\alpha_0 = \phi_{b,0}^2\left(2mL\lambda_0\left(\frac{1}{2} + \frac{4}{\pi}\frac{\phi_{f,0}}{\phi_{b,0}} + \frac{\phi_{f,0}^2}{\phi_{b,0}^2}\right) + 2c_v\frac{\phi_{f,0}^2}{\phi_{b,0}^2}\right)$ is obtained from Eq. (12).

The solution to Eq. (13b) is a damped sinusoid of initial amplitude $z_{0,\text{free}}$. This initial amplitude can be calculated from the analytical solution to Eq. (13a) at time $t = L/v$. Considering the system initially at rest, analytical solution of Eq. (13a) gives:

$$z_0(t) = -\frac{F}{\alpha_0}\frac{\phi_{b,0}}{(\lambda_0^2 + \Omega^2)}\left(\left(e^{\lambda_0 t} - 1\right)\left(\lambda_0^2 + \Omega^2\right)\frac{\phi_{f,0}}{\lambda_0\phi_{b,0}} + e^{\lambda_0 t}\Omega - \lambda_0 sin\Omega t - \Omega cos\Omega t\right), \quad 0 \leqslant t \leqslant L/v \tag{14}$$

Then, when the load leaves the beam at precise time $t = L/v$;

$$\begin{aligned} z_{0,\text{free}} &= z_0\left(\frac{L}{v}\right) \\ &= -\frac{\phi_{b,0}F}{\alpha_0(\lambda_0^2 + \Omega^2)}\left(\left(e^{\frac{\lambda_0 L}{v}} - 1\right)\left(\lambda_0^2 + \Omega^2\right)\frac{\phi_{f,0}}{\lambda_0\phi_{b,0}} + \Omega\left(e^{\frac{\lambda_0 L}{v}} + 1\right)\right), \quad t = L/v \end{aligned} \tag{15}$$

Due to the pair-wise conjugacy of the computed eigenpairs, the response of the studied underdamped mode becomes real-valued when the mode and its conjugate are summed. Consequently, the time history of forced and free vibration of midspan vertical displacement and acceleration can be computed as follows:

$$u_{b,0}(t) = 2\Re\left(\phi_{b,0} z_0(t)\right) \qquad 0 \leqslant t \leqslant L/v \tag{16a}$$

$$u_{b,0}(t) = 2\Re\left(\phi_{b,0} z_{0,\text{free}} e^{\lambda_0 (t - L/v)}\right) \qquad t \geqslant L/v \tag{16b}$$

$$a_{b,0}(t) = 2\Re\left(\phi_{b,0} \ddot{z}_0(t)\right) \qquad 0 \leqslant t \leqslant L/v \tag{17a}$$

$$a_{b,0}(t) = 2\Re\left(\lambda_0^2 \phi_{b,0} z_{0,\text{free}} e^{\lambda_0 (t - L/v)}\right) \qquad t \geqslant L/v \tag{17b}$$

where the eigenvalue in the complex form is $\lambda_0 = \lambda_{0r} + i\lambda_{0i}$. Thus, one can rewrite Eq. (17b) as

$$a_{b,0}(t) = 2e^{\lambda_{0r}(t - L/v)}\Re\left(\lambda_0^2 \phi_{b,0} z_{0,\text{free}} e^{i\lambda_{0i}(t - L/v)}\right) \tag{18}$$

Subsequently, the product $\lambda_0^2 \phi_{b,0} z_{0,\text{free}}$ is expressed in the exponential form with phase angle θ.

$$a_{b,0}(t) = 2e^{\lambda_{0r}(t - L/v)}\Re\left(\left|\lambda_0^2 \phi_{b,0} z_{0,\text{free}}\right| e^{i\theta} e^{i\lambda_{0i}(t - L/v)}\right) \tag{19}$$

The phase angle θ is not of relevance if one is only interested in the maximum amplitude of the damped acceleration $a_{b,0}(t)$, which can be finally written as

$$a_{b,0}(t) = 2\left|\lambda_0^2 \phi_{b,0} z_{0,\text{free}}\right| e^{\lambda_{0r}(t - L/v)} cos\left(\lambda_{0i}(t - L/v) + \theta\right) \tag{20}$$

Therefore, a closed-form expression for the peak mid-span acceleration amplitude during free vibration period can be obtained as per Eq. (21) below. It represents the maximum achievable acceleration when one load leaves the beam, and is a key result to superimpose the damped effect of consecutive loads, as it will be shown in section 3 of the paper.

$$a_{\max,\text{free},b,0} = 2\left|\lambda_0^2 z_{0,\text{free}} \phi_{b,0}\right| = 2F\left|\frac{\lambda_0^2\left(\left(e^{\frac{\lambda_0 L}{v}} - 1\right)\left(\lambda_0^2 + \Omega^2\right)\frac{\phi_{f,0}}{\lambda_0\phi_{b,0}} + \Omega\left(e^{\frac{\lambda_0 L}{v}} + 1\right)\right)}{\left(2mL\lambda_0\left(\frac{1}{2} + \frac{4}{\pi}\frac{\phi_{f,0}}{\phi_{b,0}} + \frac{\phi_{f,0}^2}{\phi_{b,0}^2}\right) + 2c_v\frac{\phi_{f,0}^2}{\phi_{b,0}^2}\right)\left(\lambda_0^2 + \Omega^2\right)}\right| \tag{21}$$

The approximation of Eq. (21) to the exact values will be discussed in section 2.5.3 of the paper, where a very good agreement will be shown. It should be noted that, Eq. (21) can be also used for displacement instead of acceleration, simply by removing λ_0^2.

2.5. Verification

In this section, the accuracy of the proposed discrete model and closed-form expressions is verified against the analytical solution for non-proportionally damped continuous beams with general end conditions under moving loads, developed by Svedholm et al. [23].

2.5.1. Definition of case studies

Referring to Fig. 1, four representative viscoelastically supported beam bridges of spans $L = \{8, 12, 16, 20\}$ m are considered. The mass per unit length m and the flexural rigidity EI were assumed to vary with span length L and estimated based on collected data from existing single-track ballasted concrete bridges [27], see Table 1. According to reference standards (Eurocode 1 [15]), for prestressed concrete bridges of span longer than 20 m the structural damping should be taken equal to $\xi_b = 1\%$ in a dynamic analysis. A progressive increase of damping is envisaged in [15] for the shorter spans, but in what follows a constant $\xi_b = 1\%$ will be used in all spans for simplicity.

The selected beam bridges are assumed to be supported by a shallow foundation, underlying by a homogenous half-space. The shear wave velocity of the subsoil is assumed to be $V_s = 350$ m/s, which is a realistic subsoil stiffness in the case of shallow foundations. Poisson's ratio and mass density of the soil medium are assumed constant at $\nu_s = 1/3$ and $\rho_s = 1800$ kg/m^3, respectively. Identical 3.5 × 7 m^2 rigid massless foundations are considered. The dynamic stiffness of the foundation-soil system, $k_v(\omega)$, and corresponding damping coefficient, $c_v(\omega)$, are generally frequency-dependent variables and represented as impedance functions. However, the frequency dependent impedance functions can indeed often be reasonably approximated by frequency independent ones. In the case of a shallow foundation with practical dimensions ($L_f/B_f = 2$ to 3) supported by a unsaturated homogenous half-space, the vertical dynamic stiffness and radiation damping coefficients of the studied foundation-soil system can be approximated by their static values ($\omega \approx 0$) using the following equations [28,29].

$$k_v \approx \frac{\rho_s V_s^2 A_f}{2B_f(1 - \nu_s)}\left(0.73 + 1.54\left(\frac{B_f}{L_f}\right)^{0.75}\right) = 3.8\,\text{GN/m} \tag{22}$$

$$c_v \approx \rho_s \frac{3.4V_s}{\pi(1 - \nu_s)}A_f = 25\,\text{MN.s/m} \tag{23}$$

where V_s is the shear wave velocity of the soil layer and B_f, L_f and A_f are the semi-width, semi-length and the area of the foundation, respectively.

In the case of foundations underlain by layered soil stratum or of pile groups, the impedance functions are strongly frequency dependent and using static values can fail. Nevertheless, when the resonant response of

Table 1
Cross-sectional data for studied single-span beam bridges.

L (m)	8	12	16	20
m (ton/m)	9.99	12.31	14.63	16.95
EI (GNm^2)	5.68	12.55	22.56	36.05
$f_{0,SS}$* (Hz)	18.51	11.01	7.62	5.73

* The natural frequency of the simply-supported (SS) beam on rigid supports.

the structural system is predominantly governed by its fundamental mode, as in the case of the studied system, the constant values for k_v (ω_0) and c_v (ω_0), computed at ω_0, can be used [22]. Since the fundamental frequency of the studied system itself depends on k_v and c_v, an iterative procedure should be used to calculate the constant values for k_v (ω_0) and c_v (ω_0). The general steps of the iterative procedure can be summarized as follows:

1. Initial estimation of the fundamental natural frequency of the system, ω_0, as equal to the natural frequency of the corresponding simply supported beam, $\omega_{0,SS}$.
2. Pick constant values for spring stiffness $k_v(\omega_0)$ and dashpot coefficient $c_v(\omega_0)$ from frequency-dependent impedance function at the discrete frequency point ω_0.
3. Compute the updated fundamental natural frequency of the system using $k_v(\omega_0)$ and $c_v(\omega_0)$ through closed-form expression in Eq. (6).

The procedure repeats steps 2 to 3 until convergence is achieved.

2.5.2. Fundamental modal characteristics

A comparison between computed complex modal characteristics of the 1st vertical bending mode of the studied cases are presented in Table 2. As can be seen, the calculated undamped natural frequency and modal damping ratio using the closed-form expressions in Eq. (6) and Eq. (8) are in perfect agreement with the reference results from the analytical solutions.

2.5.3. Maximum free vibration and cancellation phenomena under a single moving load

A comparison between the estimated maximum free vibration amplitudes by Eq. (21) and the reference solution [23] is shown in Fig. 3. The exact results has been obtained by computing the time history of the mid-span free vibration of the corresponding continues VS beam [23] and getting the peak value at each travelling speed, considering only the fundamental vertical mode of vibration. As can be seen, the predicted peak free vibration amplitudes by the proposed closed-form expression are in a very good agreement with the reference solution. As shown in Fig. 3, the pattern of cancellation and maximum free vibration situations in the studied viscoelastically supported beams is similar to that of the simply supported or elastically supported cases in their fundamental mode [13,19]. When the load passes over the beam at a certain speed close to the cancellation condition, the amplitudes of free vibration response become very low. Conversely, between two consecutive cancellations, the maximum free vibration levels occur.

Using Eqs. (17), the variation of maximum total and maximum free vibration acceleration amplitudes for one of case study beams ($L = 12$ m), as a function of moving load speed is plotted in Fig. 4. As shown, the maximum free vibration amplitudes are generally close or even higher than the maximum forced vibration amplitudes except in the vicinity of cancellations points where the forced vibration amplitudes prevails. The computed time histories of midspan acceleration of the case study beam ($L = 12$ m), travelled by a single load at speed $v = 244$ km/h and $v = 316$ km/h, are presented in Fig. 5a and 5b, respectively. As can be seen, the predicted time histories by the approximate discrete model are in a very good agreement with the reference solution considering only the fundamental vertical mode of vibration.

Table 2
Comparison between computed fundamental modal characteristics.

L (m)	Reference solution [21]		Closed-form formula	
	f_0 (Hz)	ξ_0 (%)	$f_0^{(1)}$ (Hz)	$\xi_0^{(2)}$ (%)
8	17.81	3.65	17.83	3.63
12	10.66	2.30	10.67	2.29
16	7.42	1.73	7.43	1.73
20	5.60	1.46	5.60	1.46

(1) Eq. (6), (2) Eq. (8)

3. Approximate formula for train-induced vertical acceleration at resonance

The railway bridge decks traveled by high-speed trains may experience extreme vibration levels due to the periodic nature of the axle loads, particularly under resonance condition [14]. Resonance occurs when the train load frequency coincides with a multiple of the fundamental frequency of the bridge. The j^{th} resonant speed of a railway bridge traveled by a row of equidistant loads can thus be estimated by Eq. (24) [1,6,15]:

$$v_j^r = \frac{f_0 d}{j} \tag{24}$$

where f_0 is the fundamental frequency of the bridge, d is the characteristic axle distance and j is an integer multiple that indicates the resonant sub-harmonic for $j > 1$.

Typically, the bridge deck acceleration level is the critical parameter in the case of short-to-medium span simple beam bridges [15,30–31]. Hence, it is of great interest to derive a simple formula to estimate the value of this parameter during the initial design stages. The strategy is to add the contributions of the successive passing loads at resonance, each of which generates free vibrations of amplitude given by Eq. (21). During the passage of a train of loads, the peak free vibrations, as shown in Fig. 3, may add and create a strong resonance as the spacing d between consecutive axles is such that Eq. (24) holds for some particular j. The smaller the value of j, the higher the resonance peak is to be expected. Hence, if the amplitude of the free vibrations generated by the loads will be close to or higher than its forced vibrations, as shown in Fig. 4, then a good estimation at resonance can be achieved by superimposing only the free vibrations of all the train loads. A similar approach was previously employed by Museros et al. [13] to develop an approximate formula to estimate peak vertical accelerations of simply supported beams.

3.1. Addition of free vibrations of damped amplitude (superposition factor F_S)

The total damped free vibration generated by a regular train consisting of N equidistant loads can be obtained by applying the principle of superposition. In the case of a beam traversed by a regular train at the j^{th} resonance speed, the maximum acceleration due to the combination of the free vibrations will occur when the last load has left the beam [13] and the vibration generated by this group reaches its maximum. Museros et al. [13,32] showed that the effects of N equidistant loads at the j^{th} resonance can be simply added by using the *superposition factor*, F_S, which is the particular expression of the train signature at the corresponding speed:

$$F_S(\xi_0, N, j) = \frac{e^{2\pi\xi_0 j} - e^{-2\pi\xi_0 j(N-1)}}{e^{2\pi\xi_0 j} - 1} \tag{25}$$

For very high values of N, the maximum F_s is obtained as the second term in the numerator of Eq. (25) approaches zero. In this way, an asymptotic value, $F_{s,max}(\xi_0,\infty, j)$ that provides a measure of the maximum expected intensity of each subresonance j can be obtained. From Eq. (25) it can be shown that bridges where damping is lower than some 1.5–2.0% generally need to be crossed by long trains to build up resonance of the first sub-harmonics near its maximum achievable amplitude [32].

3.2. Combined effects of closely spaced loads (Bogie factor F_B)

According to Eurocode [15], train-induced vibration analysis of high-speed railway bridges should be performed using HLSM-A load

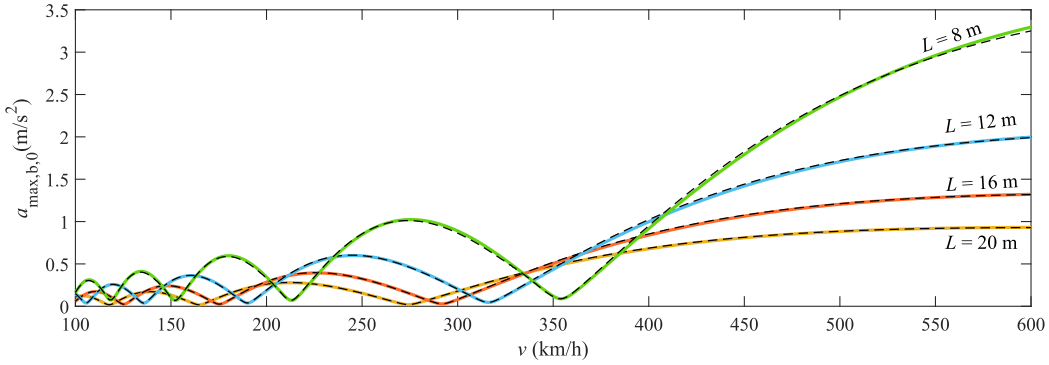

Fig. 3. Free vibration amplitude of the fundamental mode as a function of speed: Approximate formula in Eq. (19) (solid lines) , reference solutions [21] (dashed lines).

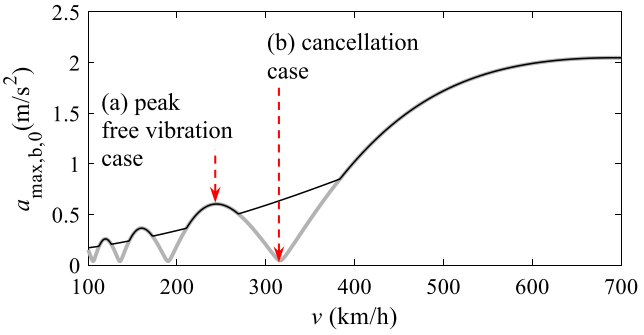

Fig. 4. Maximum vibration levels due to a single load passing over VS beam (L = 12 m). Overall maximum (black solid line); maximum during the free vibration period (grey solid line).

models. HLSM-A train models belong to the type of articulated trains, which share a bogie located between each pair of coaches. Hence, the repetitive loads which generates resonance are set in pairs. Generally, in the case that the loads are arranged in closely spaced pairs, there will be only a slight decay of structural vibration between consecutive loads in each bogie [13]. As shown by Museros et al. [32] and other researchers (see [32] and the references therein), the effects of two consecutive loads in one bogie travelling at speed v can be represented exactly by the spectrum or signature of the bogie, which here will be referred to as *Bogie factor*, F_B, defined in Eq. (26). This factor take values between zero (perfect bogie cancellation by subtraction of the effects of each axle) and two (perfect in-phase addition, or bogie resonance).

$$F_B(b,\omega_0,\xi_0,v)=\sqrt{1+e^{-2b\xi_0\omega_0/v}+2e^{-b\xi_0\omega_0/v}cos\frac{b\omega_0}{v}} \tag{26}$$

where b is the bogie wheelbase.

3.3. Maximum vertical acceleration at resonance under articulated train load models

Finally, by combining Eqs. (21), (25) and (26), an approximate closed-form expression is derived to estimate the maximum mid-span acceleration due to resonance of the fundamental mode of a VS beam passing by an articulated train.

$$a_{res}=a_{max,free,b,0}F_S(\xi_0,N,j)F_B(b,\omega_0,\xi_0,v) \tag{27}$$

As will be shown in section 4.1 and 4.2, there may be some circumstances when the true maximum acceleration is achieved during the forced vibration period. Besides, as the power cars and the end passenger coaches interrupt the repetitive pattern of intermediate passenger cars, the peak response due to the combination of the free vibrations may not occur exactly when the last load leaves the bridge. However, the major part of the response in case of resonance will be generated by the repetitive passenger coaches, and this effect will be captured by Eq. (27). Thus, the estimated values by Eq. (27) are still valuable and reasonable for a preliminary dynamic assessment of beam bridges considering SSI. Because in certain cases $F_{s,max}$ will only be grasped by larger number of N, for practical applications it may be on the safe side to artificially increase the number of N, avoiding underestimation of resonant peaks using Eq. (27).

As a more accurate and versatile alternative, the maximum acceleration can be estimated by the LIR method [14] using the full train spectrum (signature) as per Eq. (28).

$$a_{res}=a_{max,free,b,0}G(d_i,v,\omega_0,\xi_0) \tag{28}$$

In Eq. (28), the term $G(d_i,v,\omega_0,\xi_0)$ is the train spectrum with constant unit axle loads (F_i = 1) and has the following form:

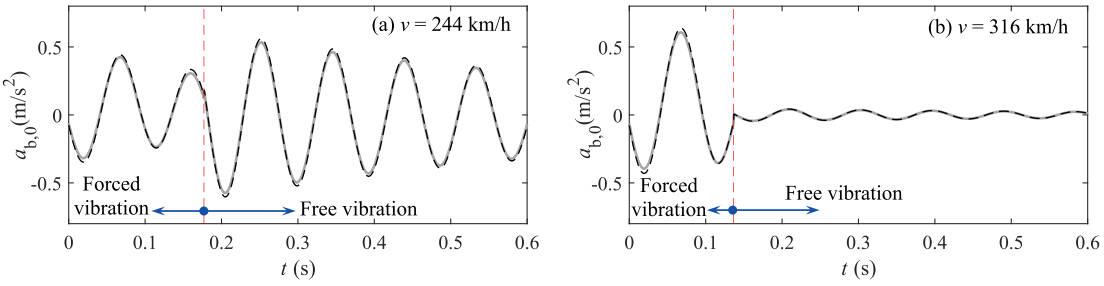

Fig. 5. Midspan acceleration time histories of a VS beam (L = 12 m) travelled by a single load F = 100 kN. Reference solution [21] (– – –), approximate discrete model Eqs. (17) (grey solid line).

$$G(\omega_0,\xi_0,d_i,v)=\sqrt{\left(\sum_{i=1}^{k}cos\left(\frac{\omega_0(d_k-d_i)}{v}\right)e^{-2\xi_0\omega_0(d_k-d_i)/v}\right)^2+\left(\sum_{i=1}^{k}\sin\left(\frac{\omega_0(d_k-d_i)}{v}\right)e^{-2\xi_0\omega_0(d_k-d_i)/v}\right)^2} \quad (29)$$

where k is the total number of loads in the train and every d_i(m) distance associated to each axle load which is measured from the first load, in such a way that $d_1 = 0$.

Using Eq. (28), the effect of different characteristic axle distances between coaches and locomotives on the resonance phenomenon can be considered—providing that Eq. (29) applies for all possible subtrains. Although the LIR method is more versatile than the proposed approximate formula in Eq. (27), its mathematical expression is rather involved and thus deriving a closed-form expression for $G(d_i,v,\omega_0,\xi_0)$ becomes unfeasible.

3.4. Influence of shear deformation and additional bending modes:

Because the approximate formula proposed in subsection 3.3 is based on the contribution of the fundamental bending mode obtained from Bernoulli-Euler beam theory, a discussion is deserved regarding the potential influence of both shear deformation and additional longitudinal bending mode shapes.

The resonant vibration of SS, single-track railway bridges with non-skewed supports is governed by longitudinal bending modes as long as the deck has a vertical symmetry plane that contains the axis of the track. In those structures, loading takes place in that symmetry plane and excitation of the torsion modes is only due to track irregularities, providing that the (elastic or rigid) supports are also symmetric. Since this article is focussed specifically in the appearance of resonant vibration, track irregularities are disregarded. Other less relevant effects capable of exciting torsional or transverse modes, such as rolling or yawing motions of the sprung masses, are also neglected.

Even if only longitudinal bending modes prevail, damping ratios of the various modes could be significantly different, which is of great importance for assessing the maximum levels of vibration. The following tables show some representative results for the examples described in section 2.5: Tables 3-5 present a comparison between modal properties for different beam theories, based on the finite element solution using commercial software COMSOL v5.6 [33]. The beams are discretized using quadratic elements with an element sized of 0.5 m.

Table 3 shows a comparison between computed fundamental modal properties and the estimated error between solutions based on different beam theories. As can be seen, considering the shear deformation using Timoshenko beam theory generally lowers the fundamental frequency and modal damping ratios. However, the difference between computed fundamental frequency and damping ratios for the studied short-span VS beams based on the two theories is negligible (around 1–2%).

Table 3
Comparison between computed fundamental modal properties of studied VS beams based on different beam theories using FE.

L (m)	Bernoulli-Euler theory				Timoshenko Theory		Timoshenko/B-E error	
	Closed-form formula		FE-solution		FE-solution			
	f [1] (Hz)	ξ [2] (%)	f (Hz)	ξ (%)	f (Hz)	ξ (%)	Δf (%)	$\Delta\xi$ (%)
8	17.83	3.63	17.81	3.65	17.6	3.57	−1.2	−2.2
12	10.67	2.29	10.66	2.30	10.57	2.26	−0.8	−1.7
16	7.43	1.73	7.42	1.73	7.36	1.71	−0.8	−1.2
20	5.60	1.46	5.6	1.46	5.56	1.45	−0.7	−0.7

[1] Eq. (6).
[2] Eq. (8).

Table 4
Comparison between computed higher order modal properties of short-span VS beam ($L = 8$ m) based on different beam theories using FEA.

Mode	Bernoulli-Euler theory		Timoshenko Theory		Timoshenko/ B-E error	
	f (Hz)	ξ (%)	f (Hz)	ξ (%)	Δf (%)	$\Delta\xi$ (%)
1st bending	17.81	3.65	17.6	3.57	−1.2	−2.2
2nd bending	72.4	8.35	69	7.78	−4.7	−6.8
3rd bending	166.1	8.77	149.9	7.7	−9.8	−12.2

Table 5
Comparison between computed higher order modal properties of short-span VS beam ($L = 12$ m) based on different beam theories using FEA.

Mode	Bernoulli-Euler theory		Timoshenko Theory		Timoshenko/B-E error	
	f (Hz)	ξ (%)	f (Hz)	ξ (%)	Δf (%)	$\Delta\xi$ (%)
1st bending	10.66	2.3	10.57	2.26	−0.8	−1.7
2nd bending	42.4	8.04	40.8	7.51	−3.8	−6.6
3rd bending	97.9	9.62	90	8.58	−8.1	−10.8

Moreover, Tables 4 and 5 present a comparison between computed higher-order modal properties of the short-span VS beams ($L = 8$ m & $L = 12$ m) and the estimated error between solutions based on different beam theories. As expected, the effect of shear deformation on the modal properties of higher order modes with higher frequencies becomes more important. However, in the presence of viscoelastic supports and non-proportional damping, these higher order modes are much more damped than the fundamental mode of vibration and consequently their contribution to the total resonant response becomes much weaker than in the case of a simply supported beam on rigid supports.

A quantification of the large difference between the amplifications at resonance expected for those modes is obtained directly from Eq. (25). For such a purpose, a train with short carriages that is able to excite sub-harmonics as close as possible to the first one is preferable. Considering a train of carriage length $d = 13.5$ m, and the natural frequencies in Table 5 for Timoshenko beam theory, one can look for realistic resonant speeds below 400 km/h by means of Eq. (24). In so doing it can be seen that the second sub-harmonic ($j = 2$) of the first mode will be reached at 257 km/h. In such case, for a train of 15 equidistant loads a resonant superposition factor $F_S = 4.0$ would be obtained. Analogously, the second mode would develop a fifth sub-harmonic ($j = 5$) at 397 km/h, with $F_S = 1.1$, which means that virtually no resonance amplification exists for the second mode. That same (augmented) situation repeats for higher sub-harmonics, and then also for the third mode—notice also that, within realistic speeds, higher sub-harmonics are favoured by longer train carriages. Therefore, higher bending modes benefit from a substantial amplitude reduction that arises from their high damping ratios.

It is also of interest to recall that previous studies have confirmed that, even for SS beams with no SSI (beams on rigid supports), the first bending mode is prevalent and provides a good estimate of the peak resonant acceleration if the same damping is assigned to all modes ([13], section 6.5).

To close subsection 3.4, it should be emphasised that the preceding conclusions are in accordance with relevant field measurements where the prevalence of the first bending mode at resonance has been observed. The well-known ballast instability problems observed in the pioneering Paris-Lyon TGV were due to resonance of the fundamental mode [14], and similar resonant behaviours were later observed in the Hanover-Wurzburg line [34] and Madrid-Sevilla lines [35]. However, in the two latter cases no destabilization of ballast was observed, but strong impact factors were recorded. Also, a field test conducted in Germany on the SS Erfttal filler beam bridge, of span 24.6 m, revealed resonant vibration at 250 km/h under the passing of an ICE-3 [36]. Recently in

Spain, a clear resonant behaviour of a 15 m SS prestressed girder bridge was monitored when a Renfe Class S103 train crossed the structure at 279 km/h [37]. That same year, a visible resonance peak was observed during the tests of a SS composite bridge of span 19.5 m under the circulation of an ICE4 [38]. These cases of strong vibration were all of them related to the fundamental bending mode. No ballast instability problems were reported.

4. Practical application and validation

In the following subsections, the accuracy and applicability of the proposed approximate formula (Eq. (27)) for estimating the maximum acceleration generated by high-speed trains is examined through comparison with the analytical solutions developed by Svedholm et al. [23]. In the following, the same case studies as defined in section 2.5.1 are used.

4.1. Maximum vertical acceleration under series of equidistant loads (regular train)

The accuracy of the proposed closed-form formula in Eqs. (27) for estimating the maximum mid-span acceleration in free vibration response after the passage of a regular train (series of N equidistant loads) is investigated here. A comparison between the exact maximum acceleration at bridge mid-span and the approximated ones by Eq. (27) is presented in Fig. 6, considering two different sets of regular trains. As mentioned in section 3.1, the maximum acceleration due to the combination of the free vibrations occurs when the last load has left the beam and the acceleration created by this group reaches its maximum [13]. Hence, for verification purposes, the maximum acceleration computed by the reference solution is picked from the free vibration period. As expected, the resonant peaks are very well estimated by the proposed formula.

Fig. 7 presents a comparison between the maximum total and maximum free vibration acceleration for two of the case study bridges. As one can expect, the total maximum acceleration does not coincide with the free vibration one for all train speeds, but the resonant peaks of the regular train are very well captured in both examples. Though some small differences are found at 390 km/h in Fig. 7a and 550 km/h in Fig. 7b, they will not be relevant for initial assessments of bridges, where Eqs. (27) and (28) will be used. Conversely, more refined and time-consuming numerical models will typically be used in the final stages of design, in order to obtain the peak responses with the greatest possible accuracy.

4.2. Maximum vertical acceleration under HSLM load models (Articulated trains)

As a particularly useful application, an estimate of the peak acceleration due to the free vibrations generated by high-speed HSLM-A load models can be obtained by applying Eq. (27). A comparison between the exact maximum total acceleration at bridge mid-span and the one approximated by Eqs. (27) is presented in Fig. 8. As shown, the predominant resonant peaks are very well approximated except for higher order resonant sub-harmonics in Fig. 8a/8b (lower speeds) and low order resonant sub-harmonics in Fig. 8c/8d (higher speeds).

In addition to the cases when the maximum acceleration of one single passing load is achieved, during the forced vibration period, the main reason for the discrepancies observed in Fig. 8 between the values approximated by Eq. (27) and the reference solution is the disregarded effect of the full train spectrum (effect of the last power car), which modifies to some extent the resonant phenomenon. But as can be seen in Fig. 8, by using the full train spectrum through the LIR method, much better agreement is achieved between the estimated peak values, Eq. (28), and the reference solution, in all peaks that are significant for a preliminary structural design.

In comparison with a full time integration of the equations of motion, it should be emphasized that Eqs. (27) as well as (28) will have much lower computational cost, which is of importance for screening various different alternatives in a particular bridge design, as well as carrying out parametric studies for series of bridges.

4.2.1. Additional validation for short spans

Because the behaviour of bridges is largely dependent on the span, it is preferable to analyse one additional example of span between 8 m and 12 m. For such short spans, the dependency of frequency on the squared length, as well the influence in the response of L/d ratios between span and coach length, will be better captured by including the results of that further example. For such purpose, a bridge of span 10 m has been selected and the results of its analysis are shown in Fig. 9. As in the previous section, it can be seen that all peak responses that may be relevant for an initial design are well captured by using the full train spectrum through the LIR method, even for the lower speeds below 200 km/h.

5. Conclusions

In this paper a novel closed-form expression for estimating the maximum free vibration amplitude of viscoelastically supported beams under single moving load has been proposed. The methodology is based on the discrete approximation of the fundamental vertical mode of a non-proportionally damped Bernoulli–Euler beam that allows the derivation of closed-form expressions for the modal properties of the system.

Having the complex modal characteristics of desired vibration mode, an analytical solution for the free vibration response of the beam under single moving load is developed using complex mode superposition.

Lastly, an approximate formula to estimate maximum mid-span acceleration of VS beams at resonance under passage of regular and articulated trains has been proposed. After extensive numerical testing, it has been proved to be a useful tool for a preliminary dynamic assessment of beam bridges, taking into account flexibility and dissipation capacity of the supporting soil-foundation system. The low computational cost of approximate formulas is essential in the initial stages of bridge design, as well as for the screening of railway bridge networks.

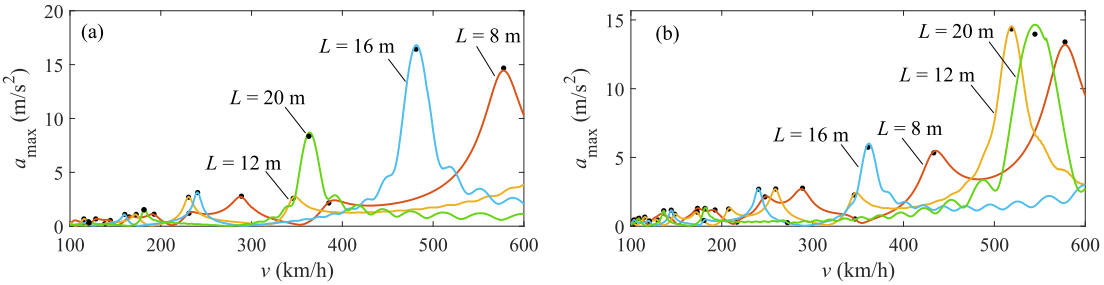

Fig. 6. Maximum vertical acceleration during free vibration period under an arbitrary regular train, (a) $N = 18$, $d = 18$ m, $F = 170$ kN, (b) $N = 11$, $d = 27$ m, $F = 210$ kN. (• a_{res} approximated by Eqs. (27) while $F_B = 1$).

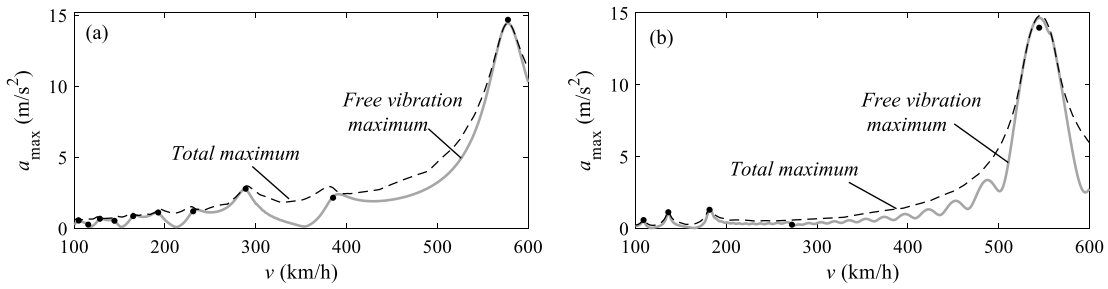

Fig. 7. Maximum vertical acceleration of a case study beam under an arbitrary regular train, (a) $L = 8$ m, $N = 18$, $d = 18$ m, $F = 170$ kN, (b) $L = 20$ m, $N = 11$, $d = 27$ m, $F = 210$ kN. (• a_{res} approximated by Eqs. (27) while $F_B = 1$).

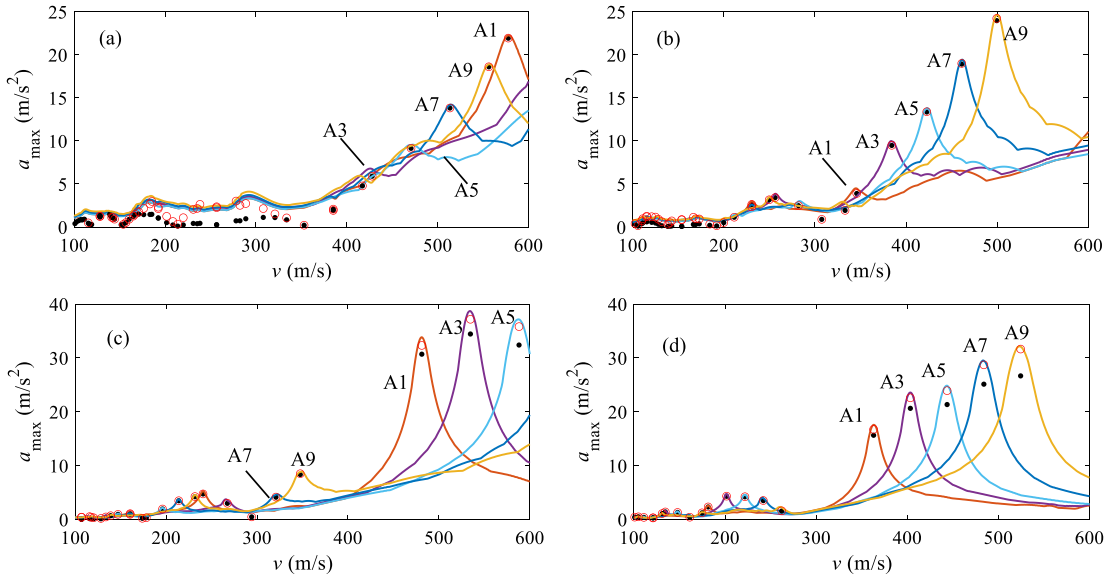

Fig. 8. Response of case study bridges to 5 HSLM-A train load models, (a) $L = 8$ m, (b) $L = 12$ m, (c) $L = 16$ m, (d) $L = 20$ m (• resonance values approximated by Eq. (27), o resonance values estimated by Eq. (28) using full train spectrum).

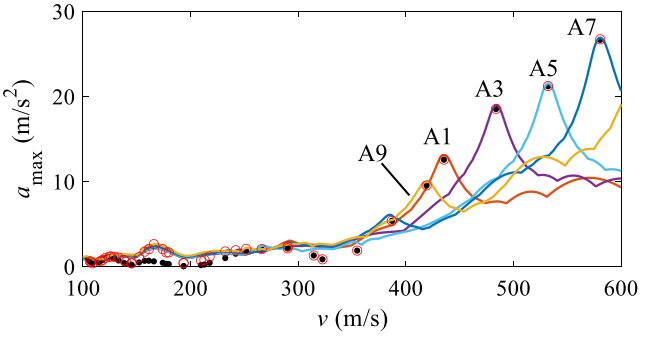

Fig. 9. Response of case study bridge $L = 10$ m to 5 HSLM-A train load models (• resonance values approximated by Eq. (27), o resonance values estimated by Eq. (28) using full train spectrum).

CRediT authorship contribution statement

Abbas Zangeneh: Conceptualization, Methodology, Software, Investigation, Formal analysis, Visualization, Writing - original draft, Validation. **Pedro Museros:** Supervision, Conceptualization, Methodology, Software, Writing - review & editing, Validation, Formal analysis. **Costin Pacoste:** Supervision, Conceptualization, Project administration, Writing - review & editing. **Raid Karoumi:** Supervision, Conceptualization, Project administration, Funding acquisition.

Declaration of Competing Interest

The author declare that there is no conflict of interest.

Acknowledgements

This research was partly sponsored by the Swedish Research Council FORMAS and has also received funding from the Shift2Rail Joint Undertaking under the European Union's Horizon 2020 research and innovation program under grant agreement No 826255 which are gratefully acknowledged.

Appendix A

In this appendix, the definition for different terms in closed-form expressions of Eq. (6), Eq. (7) and Eq. (8) are presented.

$$\gamma = \frac{mL}{k_v}, D = \frac{\pi^4 EI}{2L^3 k_v}, \beta = \frac{c_v}{k_v},$$

$$p = \frac{2\pi^2(1+D)}{(\pi^2-8)\gamma} - 1.5\left(\frac{\pi^2\beta}{(\pi^2-8)\gamma}\right)^2,$$

$$q = \frac{\pi^6}{(\pi^2-8)^3}\left(\frac{\beta}{\gamma}\right)^3 - \frac{2\pi^4}{(\pi^2-8)^2}\frac{\beta(1+D)}{\gamma^2} + \frac{4\pi^2}{(\pi^2-8)}\frac{\beta D}{\gamma^2},$$

$$\Delta_0 = (D+1)^2\gamma^2 - 6\beta^2\gamma D + \frac{12(\pi^2-8)}{\pi^2}\gamma^2 D,$$

$$\Delta_1 = 2(D+1)^3\gamma^3 + \beta^2\gamma^2 D\left(36 + \left(36 - \tfrac{432}{\pi^2}\right)D\right) - \tfrac{72(\pi^2-8)}{\pi^2}\gamma^3 D(1+D),$$

$$S = \frac{1}{2}\sqrt{-\frac{2}{3}p + \frac{2\pi^2}{3(\pi^2-8)\gamma^2}\left(\frac{\sqrt[3]{0.25\left(\Delta_1 + \sqrt{\Delta_1^2 - 4\Delta_0^3}\right)^2} + \Delta_0}{\sqrt[3]{0.5\left(\Delta_1 + \sqrt{\Delta_1^2 - 4\Delta_0^3}\right)}}\right)}$$

$$\eta = \begin{cases} +1 & \text{if } \left(-4|S|^2 - 2p - q/|S|\right) < 0 \\ -1 & \text{if } \left(-4|S|^2 - 2p - q/|S|\right) > 0 \end{cases}$$

References

[1] Frýba L. Vibration of Solids and Structures Under Moving Loads, Noordhoff International Publishing, Groningen, TheNetherlands, 1972 (3rd edited by ThomasTelford,1999).

[2] Weaver W, Timoshenko SP, Young DH. Vibration Problems in Engineering. 5th ed. New York: Wiley; 1990. p. 448–54.

[3] Olsson M. On the fundamental moving load problem. J Sound Vib 1990;145(2):299–307.

[4] Yang Y, Yau J, Hsu L. Vibration of simple beams due to trains moving at high speeds. Eng Struct 1997;19(11):936–44.

[5] Michaltsos GT. The influence of centripetal and Coriolis forces on the dynamic response of light bridges under moving vehicles. J Sound Vib 2001;247(2):261–77.

[6] Savin E. Dynamic amplification factor and response spectrum for the evaluation of vibrations of beams under successive moving loads. J Sound Vib 2001;248(2):267–88.

[7] Pesterev A, Yang B, Bergman L, Tan C. Revisiting the moving force problem. J Sound Vib 2003;261(1):75–91.

[8] Frýba L. A rough assessment of railway bridges for high speed trains. Eng Struct 2001;23:548–56.

[9] Yau J, Yang Y. Vertical accelerations of simple beams due to successive loads traveling at resonant speeds. J Sound Vib 2006;289:210–28.

[10] Yau JD, Wu YS, Yang YB. 2001, Impact response of bridges with elastic bearings to moving loads. J Sound Vib 2001;248(1):9–30.

[11] Yang YB, Lin CL, Yau JD, Chang DW. Mechanism of resonance and cancellation for train induced vibrations on bridges with elastic bearings. J Sound Vib 2004;269:345–60.

[12] Xia H, Li HL, Guo WW, De Roeck G. Vibration resonance and cancellation of simply supported bridges under moving train loads. ASCE J Eng Mech 2014;140(5). Article 04014015.

[13] Museros P, Moliner E, Martínez-Rodrigo MD. Free vibrations of simply-supported beam bridges under moving loads: Maximum resonance, cancellation and resonant vertical acceleration. J Sound Vib 2013;332(2):326–45.

[14] ERRI D-214, 1999b. Rail bridges for speeds over 200Km/h, Final Report. European Rail Research Institute (ERRI).

[15] EN1991-2, Eurocode 1, Actions on Structures. Part2: Traffic loads on Bridges, 2003.

[16] Caughey TK, O'Kelly MEJ. Effect of damping on the natural frequencies of linear dynamic systems. J Acoust Sot Am 1961;33:1458–61.

[17] Foss KA. Coordinates which uncouple the equations of motion of damped linear dynamic systems. Trans ASME J Appl Mech 1958;25:361–4.

[18] Romero A, Solís M, Domínguez J, Galvín P. Soil-structure interaction in resonant railway bridges. Soil Dyn Earthquake Eng 2013;47:108–16.

[19] Doménech A, Martínez-Rodrigo MD, Romero A, Galvín P. On the basic phenomena of soil-structure interaction on the free vibration response of beams: application to railway bridges. Eng Struct 2016;125:254–65.

[20] Svedholm C, Pacoste-Calmanovici C, Karoumi R. Modal properties of simply supported railway bridges due to soil-structure interaction. In: Conference of 5th ECCOMAS Thematic Conference on Computational Methods in Structural Dynamics and Earthquake Engineering; 2015. p. 1709–19.

[21] Zangeneh A, Battini JM, Pacoste C, Karoumi R. Fundamental modal properties of simply supported railway bridges considering soil-structure interaction effects. Soil Dyn Earthquake Eng 2019;121:212–8.

[22] A.Zangeneh, 2018, Dynamic Soil-Structure Interaction Analysis of Railway Bridges: Numerical and Experimental Results, In TRITA-ABE-DLT; Licentiate thesis 182, Stockholm (Sweden): KTH Royal Institute of Technology. Available online: http://www.diva-portal.org/.

[23] Svedholm C, Zangeneh A, Pacoste C, François S, Karoumi R. Vibration of damped uniform beams with general end conditions under moving loads. Eng Struct 2016;126:40–52.

[24] Lallement G, Inman DJ. A tutorial on complex eigenvalues, Proceedings of 13th IMAC, Nashville, TN (1995), pp. 490-495.

[25] Givens MJ. Dynamic Soil-Structure Interaction of Instrumented Buildings and Test Structures, Ph.D. Dissertation, Department of Civil and Environmental Engineering, University of California, Los Angeles, California; 2013.

[26] Zhao Y, Zhang Y. Improved complex mode theory and truncation and acceleration of complex mode superposition. Adv Mech Eng 2016;8(10):1–16. https://doi.org/10.1177/1687814016671510.

[27] Johansson C, Andersson A, Wiberg J, Ülker-Kaustell M, Pacoste C, Karoumi R. Höghastighetsprojekt-bro: Delrapport i: Befintliga krav och erfarenheter samt parameterstudier avseende dimensionering av järnvägsbroar för farter över 200 km/h. Tech. Rep. 139, KTH Brobyggnad (in Swedish); 2010.

[28] Gazetas G. 1998, Foundation vibrations. In: Fang HY, editor. Foundation Engineering Handbook. Newyork: Springer Science+Business; 1998. p. 553–93.

[29] Wolf JP. Foundation Vibration Analysis Using Simple Physical Models. Prentice Hall; 1994.

[30] Anicotte C, Schmitt P. Dynamic study of railway bridges under new reference load models for Multiple Units. SNCF, Direction of Engineering, Dpt. of Structures; 2012.

[31] Moliner E, Martínez-Rodrigo MD, Museros P. Dynamic performance of existing double track railway bridges at resonance with the increase of the operational line speed. Eng Struct 2017;132:98–109.

[32] Museros P, Andersson A, Martí V, Karoumi R. Dynamic behaviour of bridges under critical articulated trains: Signature and bogie factor applied to the review of some regulations included in EN 1991–2. J Rail Rapid Transit 2020. https://doi.org/10.1177/0954409720956476.

[33] COMSOL Multiphysics® v. 5.6. www.comsol.com. COMSOL AB, Stockholm, Sweden.

[34] Carnerero A. Comportamiento dinámico de tableros de puentes de ferrocarril de alta velocidad formados con elementos transversales a la dirección de la vía". PhD Thesis. Universidad Politécnica de Madrid, 2007.

[35] Álvarez R, Díaz J, Moreno C, Santos J, Santos y F. Conclusiones de los ensayos realizados en el "Viaducto sobre el río Tajo" en la línea de alta velocidad Madrid-Sevilla. Consideraciones para el proyecto de obras de paso en F.F.C.C. de alta velocidad. Hormigón y Acero 1999;214:131–40.

[36] Rauert T, Bigelow H, Hoffmeister B, Feldmann M. On the prediction of the interaction effect caused by continuous ballast on filler beam railway bridges by experimentally supported numerical studies. Eng Struct 2010;32:3981–8.
[37] Galvín P, Romero A, Moliner E, Martínez-Rodrigo MD. Two FE models to analyse the dynamic response of short span simply supported oblique high-speed railway bridges: Comparison and experimental validation. Eng Struct 2018;167:48–64.
[38] Firus A, Berthold H, Schneider J, Grunert G. Untersuchungen zum dynamischen Verhalten einer Eisenbahnbrücke bei Anregung durch den neuen ICE 4. VDI-Berichte 2018;2321:233–48.